

See discussions, stats, and author profiles for this publication at: <https://www.researchgate.net/publication/258045486>

# Free-radical generation from collapsing microbubbles in the absence of a dynamic stimulus

**DATASET** in THE JOURNAL OF PHYSICAL CHEMISTRY B · JANUARY 2007

Impact Factor: 3.3

---

CITATIONS

39

---

READS

278

3 AUTHORS, INCLUDING:



**Masayoshi Takahashi**

National Institute of Advanced Industrial Sci...

32 PUBLICATIONS 635 CITATIONS

SEE PROFILE



**Pan Li**

Tongji University

17 PUBLICATIONS 334 CITATIONS

SEE PROFILE

# Free-Radical Generation from Collapsing Microbubbles in the Absence of a Dynamic Stimulus

Masayoshi Takahashi,<sup>\*,†</sup> Kaneo Chiba,<sup>‡</sup> and Pan Li<sup>†</sup>

National Institute of Advanced Industrial Science and Technology (AIST), 16-1 Onogawa, Tsukuba, Ibaraki, 305-8569 Japan, and REO Laboratory Company, Ltd., 126-61 Oomagari, Higashi-Matsushima, Miyagi, 981-0502 Japan

Received: October 23, 2006; In Final Form: December 19, 2006

Free radicals are generated by the collapse of ultrasound-induced cavitation bubbles when they are forcefully compressed by dynamic stimuli. Radical generation occurs as a result of the extremely high temperatures induced by adiabatic compression during the violent collapse process. It is generally believed that extreme conditions are required for this type of radical generation. However, we have demonstrated free-radical generation from the collapse of microbubbles (diameter = <50  $\mu\text{m}$ ) in the absence of a harsh dynamic stimulus. In contrast to ultrasound-induced cavitation bubbles, which collapse violently after microseconds, the microbubbles collapsed softly under water after several minutes. Electron spin-resonance spectroscopy confirmed free-radical generation by the collapsing microbubbles. The increase of the surface charges ( $\zeta$  potentials) of the microbubbles, which were measured during their collapse, supported the hypothesis that the significant increase in ion concentration around the shrinking gas–water interface provided the mechanism for radical generation. This technique of radical generation from collapsing microbubbles could be employed in numerous engineering applications, including wastewater treatment.

## Introduction

Microbubbles are distinguished by having a diameter < 50  $\mu\text{m}$  and have important technical applications due to their tendency to decrease in size and subsequently to collapse under water. Figure 1 schematically illustrates the key differences in behavior between normal macrobubbles and microbubbles: the former rapidly rise and burst at the water surface, whereas the latter are stable for longer periods of time underwater. Microbubbles gradually decrease in size due to the dissolution of interior gases by the surrounding water, and they eventually disappear.<sup>1</sup> We have demonstrated that microbubbles can be useful in the formation of gas hydrate due to their ability to alter the nucleation condition and their efficient gaseous solubility.<sup>1</sup> The relationship between the interior gas pressure and the bubble diameter is expressed by the Young–Laplace equation:<sup>2</sup>

$$P = P_1 + 2\sigma/r$$

Here,  $P$  is the gas pressure,  $P_1$  is the liquid pressure,  $\sigma$  is the surface tension, and  $r$  is the radius of the bubble. According to Henry's law, the amount of dissolved gas surrounding a shrinking bubble increases with rising gas pressure. The area surrounding a microbubble has been shown to change its state in a pressure–temperature ( $P$ – $T$ ) diagram to favor hydrate nucleation.<sup>1</sup> This is a typical characteristic of microbubbles. In addition, we have found that free radicals are generated from collapsing microbubbles, and it is useful in several technical applications, including the decomposition of organic chemicals

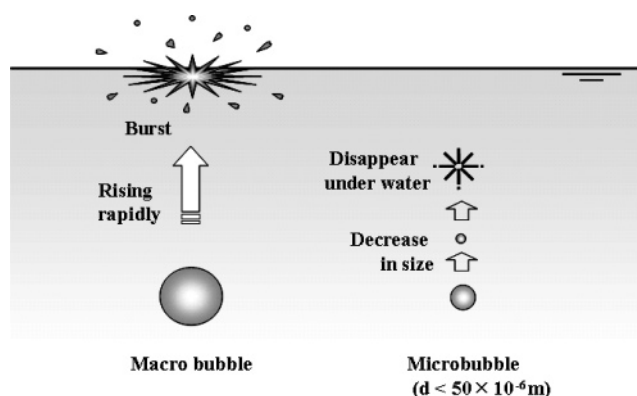


**Figure 1.** Microbubble behavior. The ordinary macrobubbles rose rapidly and burst at the surface of the water. By contrast, the microbubbles decreased in size and disappeared under the water.

and wastewater treatment. The purpose of the current study was to clarify the phenomenon of radical generation from microbubbles in the absence of dynamic stimuli, such as ultrasound or shock waves, with the aim of advancing the technical applications of this phenomenon.

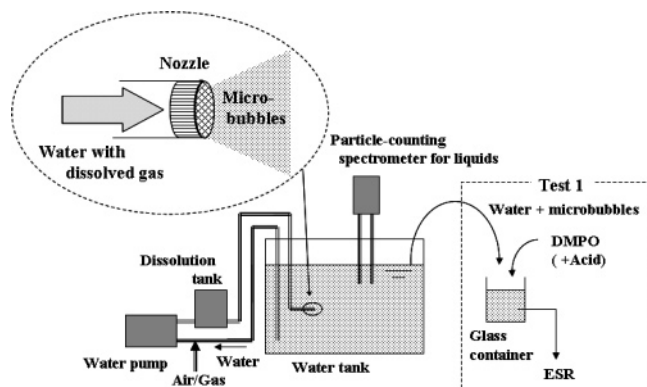
## Experimental Methods

Figure 2 shows a schematic of the microbubble generator used in this study (Awawa, Shigen-kaihatu Co., Ltd.). Water in a transparent acrylic tank was circulated by a pump through a gas-dissolution tank and a microbubble-generating nozzle. Ambient air was introduced into the circulating water at the suction side of the pump and was dissolved by means of a high-pressure system located at the discharge side. A gaseous phase of microbubbles was produced from the water supersaturated with air, due to the pressure reduction at the nozzle. Figure 3

\* To whom correspondence should be addressed. Telephone: +81-29-861-8783. Fax: +81-29-861-8496. E-mail: m.taka@aist.go.jp.

<sup>†</sup> AIST.

<sup>‡</sup> REO Laboratory Company, Ltd.



**Figure 2.** Schematic of the microbubble generator used in this study. Test 1 was conducted to confirm the radical generation by ESR measurement. To remove physical stimuli caused by microbubble generator, the sample of water was placed in a glass container prior to the mixing of DMPO with the sample.

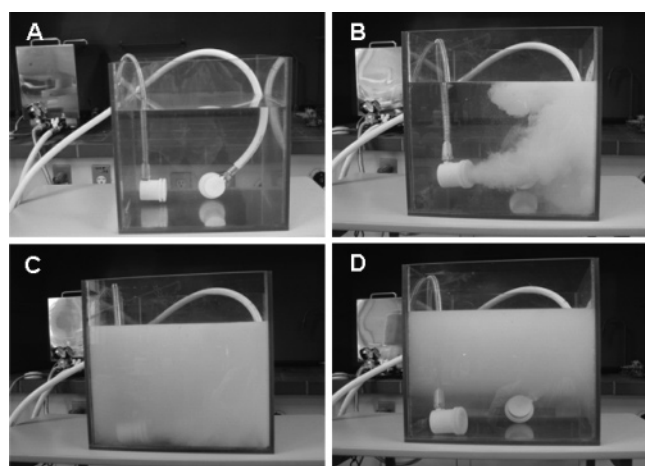


**Figure 3.** Microbubbles in a transparent acrylic tank filled with distilled water. (A) The tank is shown before the operation of the microbubble generator. (B) This is the view immediately after the operation began. (C) The condensed microbubbles gave the water a milky appearance. (D) Around 2 min after the apparatus was switched off, the water at the bottom of the tank began to become transparent again due to the rising and collapsing microbubbles. The water became fully transparent ~5 min after the generator had been switched off.

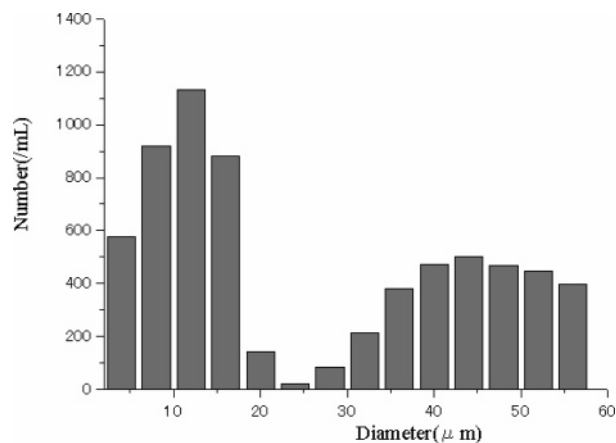


**Figure 4.** Size distribution of microbubbles measured using a particle-counting spectrometer for liquids. Two peaks were observed in this type of microbubble generator.

depicts the microbubble generator and the acrylic tank filled with distilled water. Figure 4 shows the bubble-size distribution in the water tank during the operation of the microbubble generator, as measured by a particle-counting spectrometer for

liquids (LiQuilaz-E20; Particle Measuring Systems Inc.) using a light-obscuration method. The condensed microbubbles, which were typically observed as two peaks in the distribution, gave the water in the tank a milky appearance. After the generator was deactivated, it took ~5 min for the water to return to its original state of transparency.

The study consisted of three distinct tests to confirm the phenomenon of radical generation from collapsing microbubbles. Test 1 is comprised of an electron spin-resonance (ESR) test, and test 2 and test 3 focused on the decomposition of various chemicals by the generated radicals.

**Test 1.** Many radical species are relatively reactive and, hence, typically transient, making their detection difficult on an ESR time scale. We therefore used 5,5-dimethyl-1-pyrroline-*N*-oxide (DMPO) as a spin-trap reagent. When reactive radical species are formed in the presence of this diamagnetic compound, which is undetectable by ESR, they are trapped by the reagent. The resultant stable paramagnetic nitroxyl radical adducts can be observed on an ESR spectrum.

The distilled water in the tank was tested as follows. A sample of water plus microbubbles was removed from the tank and placed in a glass container, away from physical stimuli such as hydrodynamic cavitation.<sup>3–5</sup> The electrical conductivity of the water was approximately 1.5  $\mu\text{S}/\text{cm}$ , and the temperature was approximately 20 °C. The sample was mixed with 5 mM DMPO under gentle stirring. The water, which initially had a milky appearance, was then left to stand for 10 min, by the end of which time it had become transparent. The sample was transferred to a quartz flat cell, and the ESR spectrum was measured at room temperature using an RE-2X ESR spectrometer (JEOL Ltd.) under the following conditions: microwave power = 10 mW, modulation amplitude = 0.2 mT, time constant = 1 s, and scanning time = 16 min. The hyperfine splitting constant was calibrated using  $\text{Mn}^{2+}$  as an external standard. The test was repeated with the addition of various acids, such as sulfuric acid, to the sample in the glass containers at the same time of DMPO mixing.

**Test 2.** The ability of microbubbles to generate free radicals that decompose phenol was tested in a four-stage procedure. The experimental setup of this study mimicked that shown in Figure 2, with the exception of an additional water bath to maintain the reservoir temperature below 50 °C, despite continuous operation of the microbubble generator. The water reservoir was filled with 5 L of distilled water containing 1.5 mM phenol. The ambient air supplied to the generator provided the microbubble source. The maximum pressure produced in the water circulation of the microbubble system was less than 0.4 MPa. This test was performed in the water reservoir following continuous generation of microbubbles for 3 h. In each constituent trial of the test, one of the following was added to the water reservoir prior to activation of the microbubble generator: nitric acid, sulfuric acid, and hydrochloric acid. A control in which no acid was added was also performed. Compounds that were produced during the test in the reservoir water, following addition of each acid, were analyzed by HPLC (X-LC, Jusco Co., Ltd.).

**Test 3.** Perfluorooctanoic acid (PFOA) is a material that is not decomposed by the hydroxyl radical. It has been demonstrated that sonochemical action decomposes the material via a direct pyrolysis reaction, due to extreme high temperature by adiabatic compression.<sup>6</sup> In this test 1.0 mM PFOA was added to the water reservoir to test for decomposition via the same method as described in test 2, with the addition of 3 mL of  $\text{H}_2\text{SO}_4$ . The compounds present in the reservoir water were

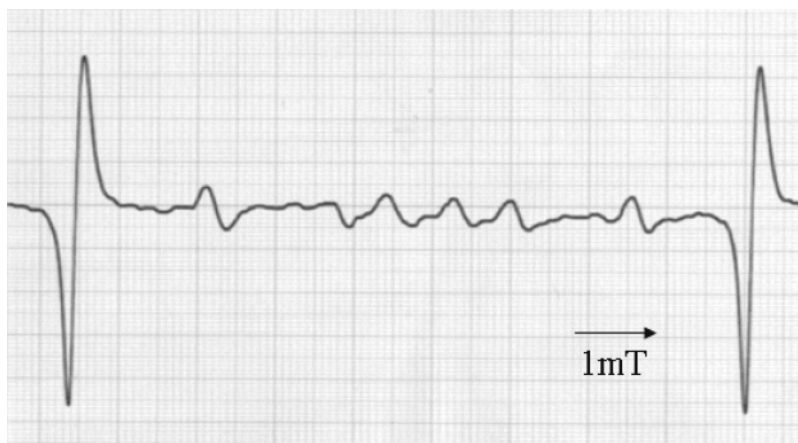


**Figure 5.** ESR spectrum of microbubbles in distilled water using DMPO as a spin-trapping reagent. The ESR spectrum was identical to that of DMPO-R, showing that alkyl radicals were generated.

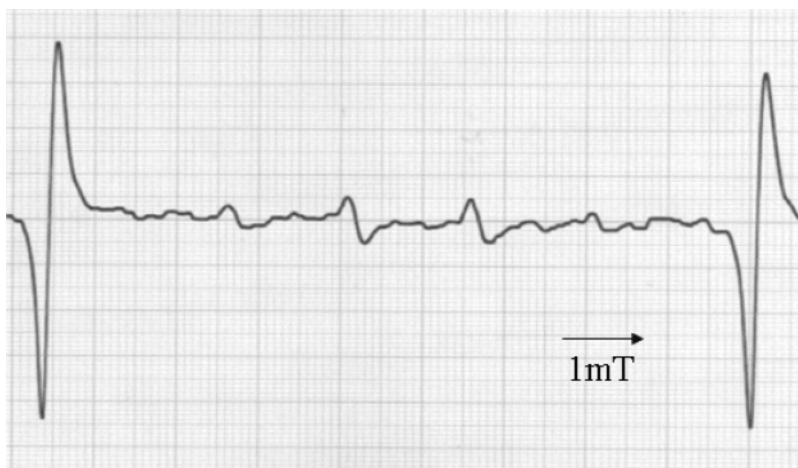


**Figure 6.** Test repeated with the addition of sulfuric acid to the water. The spectrum changed to that of DMPO-OH, indicating the production of  $\bullet\text{OH}$ .

analyzed by gas chromatography–mass spectroscopy (GCMS-QP2010, Shimadzu Co., Ltd.).

DMPO and PFOA were purchased from Tokyo Kasei Kogyo Co., Ltd., and DMPO was stored at around  $-20\text{ }^{\circ}\text{C}$ . All other chemicals were obtained from Wako Pure Chemical Industries Ltd.

## Results

**Test 1.** Figure 5 shows the ESR spectrum of the sample of distilled water from the tank. Six lines were observed after spin-trapping with DMPO, and the ESR parameters were similar to those of DMPO-R, suggesting that alkyl radicals had been generated from trace amounts of organic contaminants.<sup>7–9</sup> The ESR spectra varied depending upon the addition of acids to the water. Figure 6 shows the ESR spectrum of a sample with 0.18 M sulfuric acid ( $\text{H}_2\text{SO}_4$ ), which contains four lines (the hyperfine splitting constants of  $A_N = A_H = 14.9\text{ G}$ ) and is similar to that of DMPO-OH, suggesting that the microbubbles induced the formation of hydroxyl radicals ( $\bullet\text{OH}$ ).<sup>10–12</sup> In the absence of microbubbles, no radical generation was induced by treatment with DMPO alone or with the addition of  $\text{H}_2\text{SO}_4$ . We observed spectra identical to that derived from the  $\text{H}_2\text{SO}_4$  sample upon addition of hydrochloric acid ( $\text{HCl}$ ) and nitric acid ( $\text{HNO}_3$ ). When  $\text{NaCl}$  was added, we also observed the spectrum of DMPO-OH, which was very weak in intensity. The DMPO-R spectrum was slightly higher than that of distilled water.

**Test 2.** Prior to the test, we confirmed radical generation by adding DMPO to the water reservoir and sampling the water

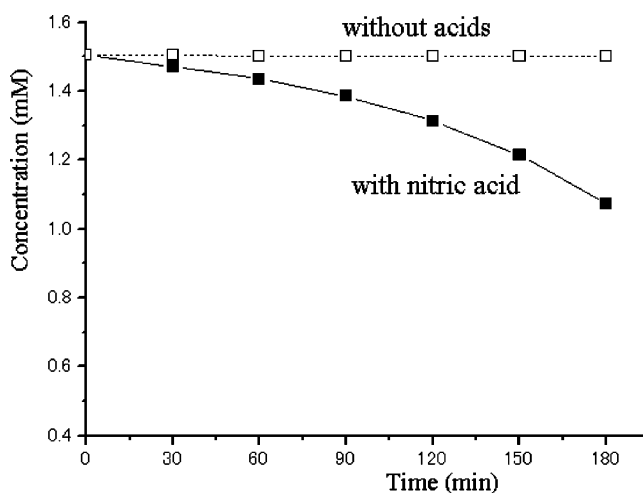


**Figure 7.** Changes in the concentrations of phenol with and without the addition of nitric acid.

for subsequent ESR measurements after the microbubble generator had been operating for 3 min. The ESR spectra were similar to those previously acquired in test 1. The primary difference was that the peak amplitudes were enhanced due to the increased amounts of free radicals produced by continuous operation of the microbubble generator.

Figure 7 shows the results of test. Without the addition of acid, we did not observe any perceptible change in the concentration of phenol after 3 h of continuous operation of



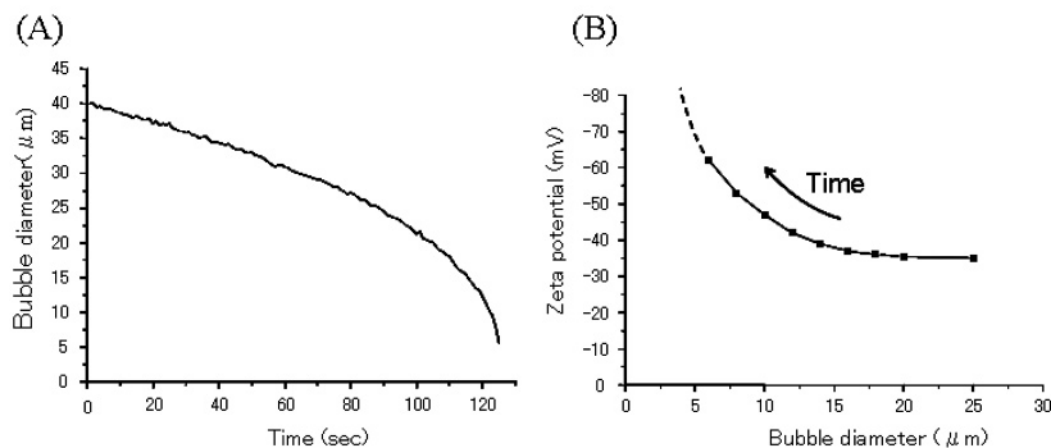


**Figure 8.** Changes in the size and  $\zeta$  potential of microbubbles over time. (A) Shown is an example of the changes in the diameter of microbubbles. The rate of shrinkage was inversely proportional to the bubble size. (B) The  $\zeta$  potential of the microbubbles was also inversely proportional to their size.

the microbubble generator. We then added 3 mL of  $\text{HNO}_3$  to the water before the next test, to generate  $\cdot\text{OH}$ , which is a stronger oxidant than the alkyl radical, from the collapsing microbubbles. About 30% of phenol was decomposed throughout the 3 h test period, and we observed the intermediate products of the phenol decomposition, such as hydroquinone, benzoquinone, formic acid, and oxalic acid.<sup>13</sup> Similar results were observed following the addition of  $\text{H}_2\text{SO}_4$  and  $\text{HCl}$ , which also resulted in  $\cdot\text{OH}$  generation.

**Test 3.** We did not observe any perceptible decomposition of PFOA throughout the 80 min test. The result indicates the microbubble collapse does not lead to “hot-spot” generation, which can be caused by acoustic and hydrodynamic cavitation.

## Discussion

It is important to consider the mechanism of free-radical generation from cavitation bubbles produced by ultrasound, to understand this process in collapsing microbubbles. When water is irradiated by a strong ultrasonic wave, numerous tiny gas bubbles appear and collapse violently, which is a phenomenon known as acoustic cavitation. These tiny bubbles repeatedly expand and contract according to the pressure oscillation of the incident ultrasonic wave. The speed of the bubble collapse increases up to the sound velocity in water, and the temperature inside a given bubble can increase dramatically due to adiabatic compression during its violent collapse. The temperature increases to  $>5000$  K during this process, and free radicals (such as  $\cdot\text{OH}$ ) are created by decomposing water vapor and noncondensable gases (including air) inside the bubbles.<sup>14–18</sup> In recent years hydrodynamic cavitation has been attempted as an alternative to acoustic cavitation.<sup>3–5</sup> When large pressure differentials are generated within a moving liquid, hydrodynamic cavitation is observed and is accompanied by a number of physical effects, such as erosion. It has been demonstrated that the chemical effects of hydrodynamic cavitation and acoustic cavitation respond identically to experimental parameters. Hydroxyl radical is generated as the dominant radical species by the extremely high temperature caused by the adiabatic compression in association with both hydrodynamic and acoustic cavitation.

The current study demonstrated free-radical generation from the collapse of microbubbles in the absence of a dynamic stimulus, such as ultrasound or large pressure differentials. The shrinking rate of the collapsing microbubbles was extremely slow compared with that of ultrasound-induced cavitation

bubbles: the microbubbles collapsed completely over a time course of tens of seconds, whereas the cavitation bubbles collapsed within microseconds. The result of test 3 indicates that PFOS was not decomposed by the collapse of microbubbles, suggesting that neither pump movement nor microbubble collapse leads to substantial increases in temperature. Further, the shrinking speed of the collapsing microbubble is not sufficiently rapid to generate an adiabatic compression. It was therefore unlikely that the mechanism of free-radical generation by microbubbles was similar to that in cavitation bubbles—the latter being related to the extremely high temperatures caused by adiabatic compression during violent collapse. It is generally accepted that radical generation requires extreme conditions, such as high temperature. Here we offer an alternate theory, based on the accumulation of ions, to explain radical generation from collapsing microbubbles.

Surface charge is an important factor in understanding the properties of microbubbles. In an electrophoresis cell, microbubbles move toward the electrode with an opposite electrical charge. The surface charge of each microbubble can be determined from the speed and direction of its movement in the presence of an electrical potential and can be evaluated by the value of the  $\zeta$  potential.<sup>19–25</sup> In distilled water, microbubbles are electrically charged to a  $\zeta$  potential of approximately  $-35$  mV. This value changes according to the precise conditions of the water. Adsorbed  $\text{OH}^-$  and  $\text{H}^+$  are crucial factors influencing the gas–water interface charge; electrolyte ions are attracted to the interface by the electrostatic force and generate an electrical double layer. The  $\zeta$  potentials of microbubbles under specific water conditions are similar, regardless of their size. Therefore, the amount of electrical charge around the gas–water interface is the same per unit area.<sup>25</sup> However, observations of collapsing microbubbles over time have shown that the  $\zeta$  potential increases according to the rate of shrinkage, which is itself inversely proportional to the bubble size (Figure 8). These observations suggest that the rate of movement of electrolyte ions in water is not sufficiently high to counteract the increasing rate of shrinkage of the microbubbles. Consequently, it is likely that some excess ions become trapped at the gas–water interface, thereby increasing its  $\zeta$  potential during the process of collapse. At present, there are insufficient data to conduct a detailed analysis. However, the accelerative increase of the  $\zeta$  potential of a microbubble suggests the extreme accumulation of ions during the final stage of the collapse process. Moreover, the extinction of the gas–water interface might cause a drastic

environmental change for the ions originally concentrated at the bubble surface. Therefore, the instantaneous high density of ions at the site of the collapsed microbubble could potentially describe the phenomenon of free-radical generation, and the exact composition of the ions that have accumulated around the interface could affect the type of free radicals generated. The drastic environmental change caused by the extinction of the gas–water interface might trigger radical generation via dispersion of the elevated chemical potential that has accumulated around the interface.

This study was conducted to verify the application of free radicals generated by collapsing microbubbles in the decomposition of an organic chemical. The microbubble collapse cannot be used as the method of degradation of PFOA, because the microbubble collapse will not lead to hot-spot generation. However, the decomposition of phenol via a hydroxyl radical reaction, without the addition of a harsh stimulus (such as ultrasound or ozone), will be important for future practical applications of microbubbles.

### Conclusions

This study demonstrated free-radical generation from collapsing microbubbles in aqueous solutions. The mechanism of radical generation differed from that of cavitation bubbles formed via incident ultrasonic waves and might have been related to ionic accumulation around the collapsing microbubbles. The decomposition of phenol by the free radicals generated without ozone or ultrasound indicated that microbubbles will be promising candidates for future practical applications.

**Acknowledgment.** We thank T. Ibusuki and K. Takeuchi for helpful discussions. We are also grateful to S. Taniguchi for assistance with data collection. This study was partly supported by the Japan Society for the Promotion of Science (Grant 14380282) and by grants from New Energy and Industrial Technology Development Organization (NEDO) and National Institute of Advanced Industrial Science and Technology (AIST) of Japan.

### References and Notes

- (1) Takahashi, M.; Kawamura, T.; Yamamoto, Y.; Ohnari, H.; Himuro, S.; Shakutui, H. *J. Phys. Chem. B* **2003**, *107*, 2171.
- (2) Carey, V. P. *Liquid–Vapor Phase–Change Phenomena*; Taylor & Francis: Bristol, U.K., 1992.
- (3) Suslick, K. S.; Mdleleni, M. M.; Ries, J. T. *J. Am. Chem. Soc.* **1997**, *119*, 9303.
- (4) Gogate, P. R.; Pandit, A. B. *Ultrason. Sonochem.* **2005**, *12*, 21.
- (5) Krishnan, J. S.; Dwivedi, P.; Moholkar, V. S. *Ind. Eng. Chem. Res.* **2006**, *45*, 1493.
- (6) Moriwaki, H.; Takagi, Y.; Tanaka, M.; Tsuruho, K.; Okitsu, K.; Maeda, Y. *Environ. Sci. Technol.* **2005**, *39*, 3388.
- (7) Utsumi, H.; Hakuda, M.; Shimbara, S.; Nagaoka, H.; Chung, Y.; Hamada, A. *Water Sci. Tech.* **1994**, *30*, 91.
- (8) Chou, D. S.; Hsiao, G.; Shen, M. Y.; Tsai, Y. J.; Chen, T. F.; Sheu, J. R. *Free Radical Biol. Med.* **2005**, *39*, 237.
- (9) Patterson, L. H.; Taiwo, F. A. *Biochem. Pharmacol.* **2000**, *60*, 1933.
- (10) Shi, X. L.; Mao, Y.; Daniel, L. N.; Saffiotti, U.; Dalal, N. S.; Vallyathan, V. *Environ. Health Perspect.* **1994**, *102*, 149.
- (11) Stan, S. D.; Woods, J. S.; Daeschel, M. A. *J. Agric. Food Chem.* **2005**, *53*, 4901.
- (12) Ueda, J.; Takeshita, K.; Matsumoto, S.; Yazaki, K.; Kawaguchi, M.; Ozawa, T. *Photochem. Photobiol.* **2003**, *77*, 165.
- (13) Sato, N.; Yamamoto, D. *Ind. Eng. Chem. Res.* **2005**, *44*, 2982.
- (14) Brennen, C. E. *Cavitation and Bubble Dynamics*; Oxford University Press: Oxford, U.K., 1995.
- (15) Leighton, T. G. *The Acoustic Bubble*; Academic Press: London, 1994.
- (16) Didenko, Y. T.; Suslick, K. S. *Nature* **2002**, *418*, 394.
- (17) Detlef, L. *Nature* **2002**, *418*, 381.
- (18) Detlef, L. *Nature* **2005**, *434*, 33.
- (19) Everett, D. H. *Basic Principles of Colloid Science*; Royal Society of Chemistry: London, 1988.
- (20) McTaggart, H. A. *Philos. Mag.* **1922**, *44*, 386.
- (21) Yoon, R.; Yordan, J. L. *J. Colloid Interface Sci.* **1986**, *113*, 430.
- (22) Li, C.; Somasundaran, P. *J. Colloid Interface Sci.* **1991**, *146*, 215.
- (23) Kim, J. Y.; Song, M. G.; Kim, J. D. *J. Colloid Interface Sci.* **2000**, *223*, 285.
- (24) Graciaa, A.; Creux, P.; Lachaise, J.; Salager, J. L. *Ind. Eng. Chem. Res.* **2000**, *39*, 2677.
- (25) Takahashi, M. *J. Phys. Chem. B* **2005**, *109*, 21858.